

Active Domain Adaptation via Clustering Uncertainty-weighted Embeddings

Viraj Prabhu¹

Arjun Chandrasekaran^{*,2}

Kate Saenko³

Judy Hoffman¹

¹Georgia Tech

²Max Planck Institute

³Boston University

Abstract

Generalizing deep neural networks to new target domains is critical to their real-world utility. In practice, it may be feasible to get some target data labeled, but to be cost-effective it is desirable to select a maximally-informative subset via active learning (AL). We study the problem of AL under a domain shift, called Active Domain Adaptation (Active DA). We empirically demonstrate how existing AL approaches based solely on model uncertainty or diversity sampling are suboptimal for Active DA. Our algorithm, Active Domain Adaptation via Clustering Uncertainty-weighted Embeddings (ADA-CLUE), i) identifies target instances for labeling that are both uncertain under the model and diverse in feature space, and ii) leverages the available source and target data for adaptation by optimizing a semi-supervised adversarial entropy loss that is complementary to our active sampling objective. On standard image classification-based domain adaptation benchmarks, ADA-CLUE consistently outperforms competing active adaptation, active learning, and domain adaptation methods across domain shifts of varying severity.

1. Introduction

Deep neural networks learn remarkably well from large amounts of labeled data but struggle to generalize this knowledge to new domains [39, 50]. This limits their real-world utility, as it is impractical to exhaustively label a large corpus of data for every problem of interest. This is particularly true in applications with abundant unlabeled data (e.g. autonomous driving), or high labeling costs (e.g. medical diagnosis). Moreover, even labeling all the available data is not a perfect solution, as a deployed model is still likely to encounter some degree of covariate shift [44]. Further, the cost of labeling is not uniform across applications, and methods that can effectively transfer the knowledge acquired from cheaper sources of labeled data (e.g., synthetic data) to a real-world target would have tremendous utility.

In practice, one could acquire labels for a subset of target instances to assist in this transfer. While Active Learning (AL) has extensively studied the problem of identify-

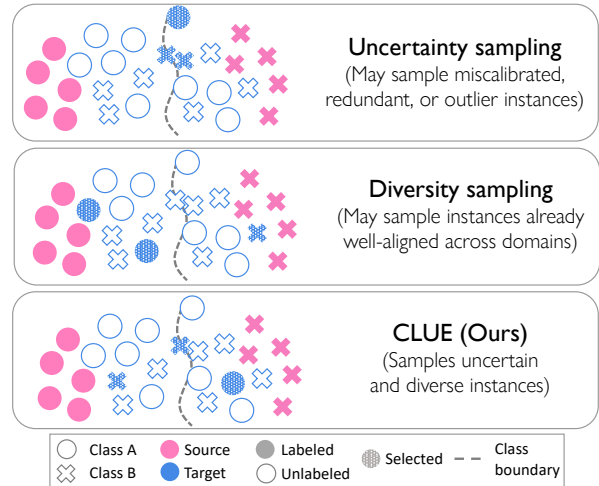


Figure 1: We address **Active Domain Adaptation** (Active DA), where the task is to adapt a source model to an unlabeled target domain by acquiring labels for selected target instances via an oracle. Prior methods in active learning based solely on uncertainty or diversity sampling do not generalize effectively to Active DA. We propose CLUE, a label acquisition strategy for Active DA that identifies instances that are both uncertain under the model and diverse in feature space, and leads to cost-effective adaptation.

ing maximally-informative instances to label [7, 43, 12, 42, 10, 2], it does not address how to effectively use either the labeled source or unlabeled target data for training. Domain adaptation (DA) however, has studied how to adapt a model trained on a labeled source domain to an unlabeled [39, 52, 13, 20] or partially-labeled [9, 55, 40] target domain. While DA may be insufficient to completely bridge a severe domain shift, it is a natural complement to AL to leverage all available data.

In this work, we study Active Domain Adaptation (Active DA) introduced by Rai et al. [36] – given labeled data in a source domain, unlabeled data in a target domain, and the ability to obtain labels for a fixed budget of target instances, the task is to select target instances for labeling and learn a model so as to maximize performance on the target test set.

Active DA presents new challenges that AL or DA do not address. In AL, labels are typically acquired for instances that are highly uncertain under the model [12, 10, 49, 24],

*Work done partially at Georgia Tech. Correspondence to: Viraj Prabhu <virajp@gatech.edu>

or diverse in a learned embedding space [42, 16]. In Active DA, label acquisition based solely on either uncertainty or diversity is suboptimal. Under a severe domain shift, uncertainty estimates on the target domain may be highly miscalibrated [47], or lead to sampling outliers or redundant instances (Fig. 1, top). Similarly, label acquisition based purely on diversity can lead to sampling uninformative instances from regions of feature space that are already well-aligned across domains (Fig. 1, middle). Clearly, an optimal label acquisition strategy for Active DA would jointly account for both uncertainty and diversity of instances.

Prior work in Active DA has also identified the importance of identifying instances that are both uncertain and diverse. The state-of-the-art method for Active DA, AADA [48] does so by selecting instances with high predictive entropy and high ‘targetness’ = $p_T(x)/p_S(x)$ under a learned domain discriminator, that they refer to as diversity. However, such targetness does not adequately ensure that selected instances are representative of the entire target distribution, or dissimilar to one another *i.e.* selected samples may be outliers or redundant. In fact, in our experiments we find that such a combination of uncertainty and diversity does not generalize to challenging domain shifts.

We propose Clustering Uncertainty-weighted Embeddings (CLUE), a novel label acquisition strategy that jointly captures uncertainty and diversity for Active DA. CLUE identifies target instances that are uncertain (informative to the model), and diverse in feature space (representative of the target data distribution). To do so, CLUE first clusters deep embeddings of target instances *weighted* by the corresponding uncertainty of the target model. To construct non-redundant batches, CLUE then selects nearest neighbors to the inferred cluster centroids for labeling. Our algorithm then leverages all available data to update the model via optimizing an adversarial entropy loss for semi-supervised DA [40], which we demonstrate to be complementary to our label acquisition strategy. We call our full method Active Domain Adaptation via Clustering Uncertainty-weighted embeddings (ADA-CLUE).

We present results on six standard image classification-based domain adaptation shifts: 4 shifts of increasing difficulty on the large and challenging DomainNet [34] benchmark, the DSLR→Amazon shift from the Office [39] benchmark, and the SVHN [31]→MNIST [26] shift from the DIGITS benchmark. ADA-CLUE improves upon the previous state-of-the art in Active DA across shifts (by as much as 10% absolute accuracy, in some cases), and also demonstrates consistent gains over state-of-the-art methods for active learning and semi-supervised DA. We analyze the robustness of our method across active sampling strategies, domain adaptation methods, model initializations, and labeling budgets. In addition, we present ablation studies of our model and analyze its behavior via visualizations.

2. Related Work

Active Learning (AL) for CNN’s. AL for CNN’s has typically focused on the batch-mode setting due to the computational inefficiency and instability associated with single-instance updates. The two most successful paradigms in AL have been uncertainty sampling and diversity sampling [2]. Uncertainty-based methods select instances with the highest uncertainty under the current model [12, 10, 49, 41], using measures such as entropy [53], minimum classification margins [37], least confidence, etc. Diversity-based methods pick a set of points that are representative of the entire dataset, and optimize for diversity in a learned embedding space, via clustering, or core-set selection [42, 16, 46, 15].

Some approaches combine these two paradigms [2, 3, 21, 57]. Active Learning by Learning [21] formulates this as a multi-armed bandit problem of selecting between coresets and uncertainty sampling at each step. Zhdanov et al. [57] propose using K-Means clustering [18] to increase batch diversity following pre-filtering based on uncertainty. A more recent example is BADGE [2], which first computes “gradient embeddings” on unlabeled points, and then runs a clustering scheme on these to construct diverse batches. In this work, we propose CLUE, a label acquisition algorithm that captures uncertainty and diversity, for the problem of active learning under a domain shift.

Domain Adaptation. The task of transferring models trained on a labeled source domain to an unlabeled [39, 52, 13, 20] or partially-labeled [9, 55, 40] target domain has been studied extensively. Initial approaches aligned feature spaces by optimizing discrepancy statistics between the source and target [52, 27], while in recent years adversarial learning of a feature space encoder alongside a domain discriminator has become a popular alignment strategy [13, 14, 51]. Recently, min-max optimization of model entropy has been shown to be effective for semi-supervised domain adaptation [40]. In this work, we apply minmax entropy optimization to achieve domain alignment for Active DA.

Active Domain Adaptation (Active DA). Rai et al. [36] first studied the task of active DA applied to sentiment classification from text data. They propose ALDA, which employs a sampling strategy based on model uncertainty and a learned domain separator. Chattopadhyay et al. [5] select target instances and learn importance weights for source points by solving a convex optimization problem of minimizing MMD between features. More recently, Su et al. [48] study Active DA in the context of CNN’s and propose AADA, an Active DA method wherein points are sampled based on their uncertainty (measured by model entropy) and targetness (measure by an adversarially trained domain discriminator), followed by adversarial domain adaptation via DANN [14]. We propose an Active DA algorithm that identifies uncertain and diverse instances for labeling followed by semi-supervised DA, that outperforms prior work across several domain shifts.

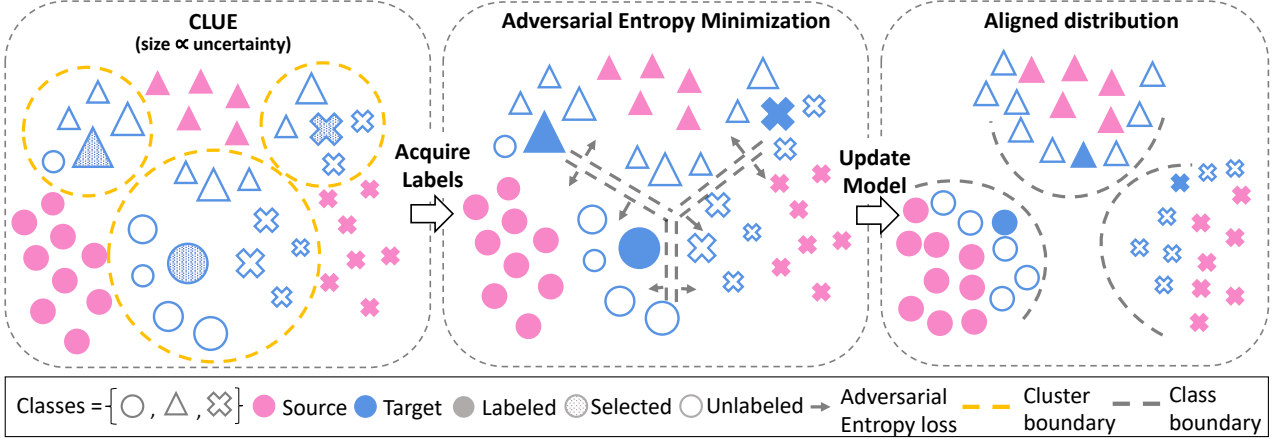


Figure 2: Our approach, Active Domain Adaptation via CLustering Uncertainty-weighted Embeddings (ADA-CLUE), acquires labels for a diverse set of target instances that are informative and representative (left). First, uncertainty-weighted embeddings of target instances, are clustered. The instance closest to each cluster centroid is then acquired for labeling, providing informative instances that are both uncertain and diverse (Eq. 10). Next, ADA-CLUE leverages the available labeled and unlabeled source and target data to update the model via a semi-supervised adversarial entropy objective (Eq. 7) (middle), which results in well-classified target data (right).

3. Approach

We address the problem of active domain adaptation (Active DA), where the goal is to generalize a model trained on a source domain to an unlabeled target domain, with the option to query an oracle for labels for a subset of target instances. While individual aspects of this problem – generalization to a new domain and selective acquisition of labels, have been well studied as the problems of Domain Adaptation (DA) and Active Learning (AL) respectively, Active DA presents new challenges. First, it is difficult to determine which target instances will, once labeled, result in the most sample-efficient domain alignment. It is also an open question as to how best to use the labeled data from the source or the unlabeled data from the target for training. Further, the optimal solutions to these questions may vary based on the properties of the specific domain shift. In this section, we present an algorithm for Active DA which performs consistently well across domain shifts of varying difficulty.

3.1. Notation

In Active DA, the learning algorithm has access to labeled instances from the source domain (X_S, Y_S) (solid pink in Fig. 2), unlabeled instances from the target domain $X_{U\mathcal{T}}$ (blue outline in Fig. 2), and a budget B ($= 3$ in Fig. 2) which is much smaller than the amount of unlabeled target data. The learning algorithm may query an oracle to obtain labels for at most B instances from $X_{U\mathcal{T}}$, and add them to the set of labeled target instances $X_{L\mathcal{T}}$. The entire target domain data is $X_{\mathcal{T}} = X_{L\mathcal{T}} \cup X_{U\mathcal{T}}$. The task is to learn a function $h : X \rightarrow Y$ (a convolutional neural network (CNN) parameterized by Θ) that achieves good predictive performance on the target. In this work, we consider Active DA in the con-

text of C -way image classification – the samples $\mathbf{x}_S \in X_S$, $\mathbf{x}_{\mathcal{T}} \in X_{\mathcal{T}}$ are images, and labels $y_S \in Y_S$, $y_{\mathcal{T}} \in Y_{\mathcal{T}}$ are categorical variables $y \in \{1, 2, \dots, C\}$.

3.2. Clustering Uncertainty-weighted Embeddings

The goal in active learning (AL) is to identify informative target instances that, once labeled and used for training the model, minimize its expected future loss. In practice, prior works in AL identify such instances based primarily on two proxy measures, uncertainty and diversity (see Sec. 2). We first revisit these terms in the context of Active DA.

Uncertainty. Prior work in AL has proposed using several measures of model uncertainty as a proxy for informativeness (see Sec. 2). However, in the context of Active DA, using model uncertainty to select informative samples presents a conundrum. On the one hand, models benefit from initialization on a related source domain, which could potentially lead to better uncertainty estimates than when learning from scratch. On the other hand, under a strong distribution shift, model uncertainty may often be miscalibrated [47]. Unfortunately however, without access to target labels, it is impossible to evaluate the reliability of model uncertainty!

Diversity. Acquiring labels solely based on uncertainty often leads to sampling batches of similar instances with high redundancy, or to sampling outliers. A parallel line of work in active learning instead proposes sampling *diverse* instances that are representative of the unlabeled pool of data. Several definitions of “diverse” exist in the literature: some works define diversity as coverage in feature [42] or “gradient embedding” space [2], while prior work in Active DA measures diversity by how “target-like” an instance is [48]. In Active DA, training on a related source domain (optionally followed

by unsupervised domain alignment), results in some classes being better aligned across domains than others. Thus, in order to be cost-efficient it is important to avoid sampling from already well-learned regions of the feature space. However, purely diversity-based AL methods are unable to account for this, and lead to sampling redundant instances.

While sampling instances that are either uncertain or diverse may be useful to learning, an optimal label acquisition strategy for Active DA would ideally capture both jointly. We now introduce CLUE, a label acquisition strategy for Active DA that captures both uncertainty and diversity.

CLUE: Clustering Uncertainty-weighted Embeddings. To measure informativeness we use predictive entropy $\mathcal{H}(Y|\mathbf{x}; \Theta)$ [53] ($\mathcal{H}(Y|\mathbf{x})$ for brevity), which for C -way classification, is defined as:

$$\mathcal{H}(Y|\mathbf{x}) = - \sum_{c=1}^C p_\Theta(Y = c|\mathbf{x}) \log p_\Theta(Y = c|\mathbf{x}) \quad (1)$$

In Active DA, entropy can be viewed as capturing both uncertainty and domainness, by considering an *implicit* domain classifier $d(\mathbf{x})$ [40] based on entropy thresholding¹:

$$d(\mathbf{x}) = \begin{cases} 1, & \text{if } \mathcal{H}(Y|\mathbf{x}) \geq \gamma \\ 0, & \text{otherwise} \end{cases} \quad (2)$$

where 1 and 0 denote target and source domain labels, and γ is a threshold value. The probability of an instance belonging to the target domain is thus given by:

$$p(d(\mathbf{x}) = 1) = \frac{\mathcal{H}(Y|\mathbf{x})}{\log(C)} \propto \mathcal{H}(Y|\mathbf{x}) \quad [C \text{ is constant}] \quad (3)$$

Next, we measure diversity based on feature-space coverage. Let $\phi(\mathbf{x})$ denote feature embeddings extracted from model h . We identify diverse instances by partitioning X_T into K diverse sets via a partition function $\mathcal{S} : X_T \rightarrow \{X_1, X_2, \dots, X_K\}$. Let $\{\mu_1, \mu_2, \dots, \mu_K\}$ denote the corresponding centroid of each set. Each set X_k should have a small variance $\sigma^2(X_k)$. Expressed in terms of pairs of samples, $\sigma^2(X_k) = \frac{1}{2|X_k|^2} \sum_{\mathbf{x}_i, \mathbf{x}_j \in X_k} \|\phi(\mathbf{x}_i) - \phi(\mathbf{x}_j)\|^2$ [56]. The goal is to group target instances that are similar in the CNN's feature space, into a set X_k . However, while $\sigma^2(X_k)$ is a function of the target data distribution and feature space $\phi(\cdot)$, it does not account for uncertainty.

To jointly capture both diversity and uncertainty, we propose *weighting samples based on their uncertainty* (given by Eq. 1), and compute the weighted population variance [35]. The overall set-partitioning objective is:

$$\operatorname{argmin}_{\mathcal{S}, \mu} \sum_{k=1}^K \frac{1}{Z_k} \sum_{\mathbf{x} \in X_k} \mathcal{H}(Y|\mathbf{x}) \|\phi(\mathbf{x}) - \mu_k\|^2 \quad (4)$$

¹This assumes that source instances have low predictive entropy, which is generally satisfied under supervised training.

Algorithm 1 ADA-CLUE: Our proposed Active DA method, which uses Clustering Uncertainty-weighted Embeddings (CLUE) to select points for labeling followed by a model update via semi-supervised adversarial entropy minimization.

- 1: **Require:** Neural network $h = f(\phi(\cdot))$, parameterized by Θ , labeled source data (X_S, Y_S) , unlabeled target data X_T , Per-round budget B , Total rounds R .
- 2: **Define:** Target labeled set $X_{\mathcal{L}T} = \emptyset$
- 3: Train source model Θ^1 (Eq. 6).
- 4: Adapt model to unlabeled target domain (Eq. 7).
- 5: **for** $\rho = 1$ to R **do**
- 6: **CLUE:** For all instances $\mathbf{x} \in X_T \setminus X_{\mathcal{L}T}$:
 1. Compute deep embedding $\phi(\mathbf{x})$
 2. Run Weighted K-Means until convergence (Eq. 4):
 - (a) Init. $K (= B)$ centroids $\{\mu_i\}_{i=1}^B$ (KMeans++)
 - (b) **Assign:**
 - $X_k \leftarrow \{\mathbf{x} | k = \operatorname{argmin}_{i=1, \dots, K} \|\phi(\mathbf{x}) - \mu_i\|^2\}_{\forall \mathbf{x}}$
 - (c) **Update:** $\mu_k \leftarrow \frac{\sum_{\mathbf{x} \in X_k} \mathcal{H}(Y|\mathbf{x}) \phi(\mathbf{x})}{\sum_{\mathbf{x} \in X_k} \mathcal{H}(Y|\mathbf{x})} \forall k$
 3. Acquire labels for nearest-neighbor to centroids
 - $X_{\mathcal{L}T}^{\rho} \leftarrow \{\operatorname{NN}(\mu_i)\}_{i=1}^B$
 4. $X_{\mathcal{L}T} = X_{\mathcal{L}T} \cup X_{\mathcal{L}T}^{\rho}$
- 7: **Semi-supervised DA:** Update model $\Theta^{\rho+1}$ (Eq. 7).
- 8: **Return:** Final model parameters Θ^{R+1} .

where the normalization $Z_k = \sum_{\mathbf{x} \in X_k} \mathcal{H}(Y|\mathbf{x})$. Our weighted set partitioning can also be viewed as standard set partitioning in an alternate feature space, where the density of instances is artificially increased proportional to their predictive entropy. Intuitively, this emphasizes representative sampling from uncertain regions of the feature space.

In practice, we approximately optimize Eq. 4 using a Weighted K-Means algorithm [22] (see Algorithm 1 – uncertainty-weighting is used in the update step). We set $K = B$ (budget), and use activations from the penultimate CNN layer as $\phi(\mathbf{x})$. After clustering, to select representative instances (*i.e.* non-outliers), we acquire labels for the nearest neighbor to the weighted-mean of each set μ_k in Eq. 4. Note that Eq. 4 equivalently maximizes the sum of squared deviations between instances in different sets [25], ensuring that the constructed batch of instances has minimum redundancy. **Trading-off uncertainty and diversity.** CLUE captures an implicit tradeoff between model uncertainty (via entropy-weighting) and feature-space coverage (via clustering). Consider the predictive probability distribution for instance \mathbf{x} :

$$p_\Theta(Y = c|\mathbf{x}) = \sigma \left(\frac{h(\mathbf{x})}{T} \right) \quad (5)$$

where σ denotes the softmax function and T denotes its

temperature. We observe that by modulating T , we can control the uncertainty-diversity tradeoff. For example, by increasing T , we obtain more diffuse softmax distributions for all points leading to similar uncertainty estimates across points; correspondingly, we expect diversity to play a bigger role. Similarly, at lower values of T we expect uncertainty to have greater influence. We treat T as a hyperparameter that may be tuned using a small validation set.

Our full label acquisition approach, Clustering Uncertainty-weighted Embeddings (CLUE), thus identifies instances that are both uncertain and diverse (Fig. 2, *left*).

3.3. Semi-supervised Domain Adaptation

Given labeled samples from the source and (a subset of) the target domain, we first compute the total cross-entropy loss \mathcal{L}_{TCE} of model h over the available labeled data.

$$\begin{aligned} \mathcal{L}_{TCE} = & \lambda_S \mathbb{E}_{(\mathbf{x}, y) \in (X_S, Y_S)} [\mathcal{L}_{CE}(h(\mathbf{x}), y)] \\ & + \lambda_T \mathbb{E}_{(\mathbf{x}, y) \in (X_{\mathcal{T}}, Y_{\mathcal{T}})} [\mathcal{L}_{CE}(h(\mathbf{x}), y)] \end{aligned} \quad (6)$$

where λ_S and λ_T are scalar weights, and \mathcal{L}_{CE} denotes the cross-entropy loss. In addition, the source and target domains are aligned via an additional objective that uses target unlabeled data. We use the minimax entropy (MME) approach for semi-supervised domain adaptation from Saito et al. [40].

Consider that model $h : X \rightarrow Y$ is composed of a feature extractor $\phi_\alpha(\mathbf{x}) : X \rightarrow Z; Z \in \mathbb{R}^M$ and classifier $f_W : Z \rightarrow Y$. Overall, the model's prediction is $p_\Theta(Y|\mathbf{x}) = \sigma(f(\phi(\mathbf{x})))$ where α and W are parameters for ϕ and f respectively, and σ denotes the softmax function. In MME, the classifier weights W are updated to maximize model entropy (Eq. 1) over target instances, and parameters of the feature extractor α are updated to minimize it. The full learning objective is given by:

$$\begin{aligned} \operatorname{argmin}_W \mathcal{L}_{TCE} - \lambda_H \sum_{\mathbf{x} \in X_{\mathcal{T}}} \mathcal{H}(Y|\mathbf{x}) \\ \operatorname{argmin}_\alpha \mathcal{L}_{TCE} + \lambda_H \sum_{\mathbf{x} \in X_{\mathcal{T}}} \mathcal{H}(Y|\mathbf{x}) \end{aligned} \quad (7)$$

where λ_H is a loss weight hyperparameter.

CLUE and MME. Our label acquisition strategy (CLUE) and domain alignment strategy (MME) complement one another. First, MME provably minimizes domain divergence under the same implicit domain classifier formulation presented in Eq. 2. Further, MME minimizes target entropy, which has the effect of producing a feature space where similar points are more tightly clustered (see Fig. 2, *middle*). This makes it easier to sample diverse points with CLUE. However, unlike minimizing entropy over all target instances, minimax entropy optimization does not push target entropy values to zero, and hence entropy of target points may still be used as a discriminative signal for sample selection ².

²See ENT vs Ours in Fig 6b, Saito et al. [40] for supporting evidence.

We call our entire active adaptation approach Active Domain Adaptation via Clustering Uncertainty-weighted Embeddings (ADA-CLUE, see Algorithm 1). Given a model trained on labeled source instances, we align its representations with unlabeled target instances via unsupervised domain adaptation. For R rounds with per-round budget B , we then iteratively i) acquire labels for B target instances that are identified via our proposed sampling approach (CLUE), and ii) Update the model using the semi-supervised domain alignment strategy described above (Eq. 7).

4. Experiments

We begin by evaluating the performance of our active domain adaptation method (ADA-CLUE) across 6 domain shifts of varying difficulty (Sec 4.1). To demonstrate the importance of each component of our method, we next present ablations of our sampling strategy (CLUE) and our choice of semi-supervised adaptation (Sec 4.2). For all experiments, we follow the standard batch active learning setting [4], in which we perform multiple rounds of batch active sampling, label acquisition, and model updates. As our performance metric, we compute model accuracy on the target test split versus the number of labels used from the target train split at each round. We run each experiment 3 times and report accuracy mean and 1 standard deviation.

4.1. Performance on the active adaptation task

DomainNet [34] is the largest domain adaptation benchmark for image classification, containing 0.6 million images belonging to 6 distinct domains spanning 345 categories. We report performance on four shifts of increasing difficulty as measured by source→target transfer accuracy: Real→Clipart (easy), Clipart→Sketch (moderate), Sketch→Painting (hard), and Clipart→Quickdraw (very hard). We use a ResNet34 [19] CNN, and perform 10 rounds of Active DA with per-round budget = 500 instances (total of 5000 labels). In addition, we evaluate performance on the SVHN [31]→MNIST [26] and DSLR→Amazon [39] shifts used in Su et al. [48]. On DIGITS, we use a modified LeNet architecture [20], and perform 30 rounds of active DA with B=10. On Office, we use a ResNet34 CNN, perform 10 rounds, and set B=30. For CLUE, we use penultimate layer embeddings, implement weighted K-means with $K = B$, and use a softmax temperature of 0.1 (selected via grid search over a small val set, see appx.) on DomainNet and 1.0 on other shifts. For training details see appendix.

Baselines. We compare our method against four baselines: State-of-the-art methods for active domain adaptation (AADA [48]), semi-supervised DA (SSDA-MME* [40]), active learning (BADGE [2]), and a simple baseline of uniform sampling with finetuning (uniform + finetuning (FT)). We describe the three state-of-the-art methods below.

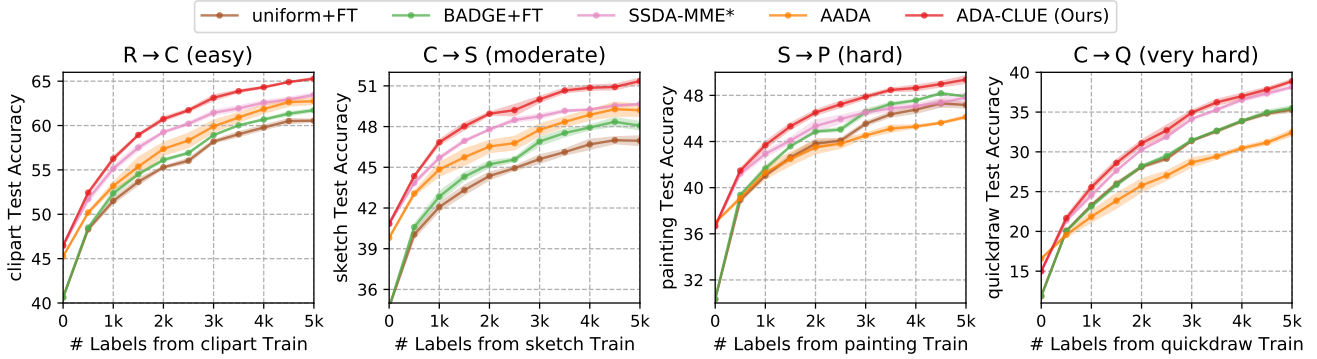


Figure 3: Active DA accuracy across 4 shifts of increasing difficulty from DomainNet [34], over 10 rounds with per-round budget $B = 500$: ADA-CLUE consistently outperforms a state-of-the-art active learning (BADGE [2]), semi-supervised DA (MME [40]), and active DA (AADA [48]) method.

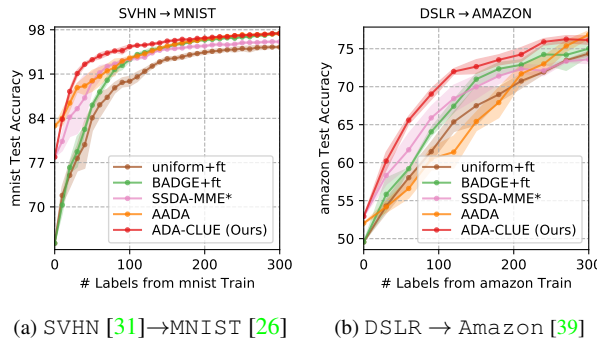


Figure 4: Active DA performance on DIGITS and Office.

(i) AADA: Active Adversarial Domain Adaptation [48] performs alternate rounds of active sampling and adversarial domain adaptation via DANN [14]. It samples points with high predictive entropy and high probability of belonging to the target domain as predicted by the domain discriminator. **ii) SSDA-MME*:** [40] The model is optimized via the semi-supervised MME loss on randomly sampled target points. The asterisk denotes that for simplicity and fair comparison against baselines, in our implementation we do not use a similarity-based classifier or L2-normalize features³. **iii) BADGE + finetuning (ft):** Batch Active Learning by Diverse Gradient Embeddings [2] is a recently proposed, state-of-the-art active learning strategy that constructs diverse batches by running KMeans++ [1] on “gradient embeddings” that incorporate model uncertainty and diversity. The model is then finetuned on acquired labels.

All baseline models are first initialized with pretrained ImageNet weights and then trained to completion on the labeled source domain. SSDA-MME*, AADA, and ADA-CLUE additionally employ unsupervised feature alignment to the

³We report results on all 345 classes in DomainNet instead of the 126-class subset that Saito et al. [40] use.

target domain, which leads to a higher initial performance.

Results. Fig. 3 and 4 demonstrate our results on DomainNet, DIGITS, and Office. ADA-CLUE consistently outperforms alternative methods across shifts and rounds. For instance, on the Clipart→Sketch (Fig. 3, C→S) shift, we improve upon the state-of-the-art AADA active DA method by 2-4% over rounds. This demonstrates the benefit of jointly capturing uncertainty and diversity for active sampling in combination with strong semi-supervised feature alignment. We observe similar improvements on the DIGITS (Fig. 4a) and Office (Fig. 4b) benchmarks, seeing as much as 10% higher accuracy than AADA at some rounds on the latter.

On DomainNet, we find that the performance gap between ADA-CLUE and AADA [48] increases with increasing shift difficulty (> 6% improvement on the very hard C→Q shift). As discussed in Sec. 3, the optimal label acquisition criterion may vary across different shifts and stages of training as the model’s uncertainty estimates and feature space evolve, and it is challenging for a single approach to work well across all settings. However we find that ADA-CLUE is able to effectively trade-off uncertainty and feature-space coverage and perform well even on difficult shifts.

Across shifts, we find that SSDA-MME* [40] is closest to ADA-CLUE in terms of performance. This is unsurprising since Mittal et al. [30] show that the benefit of deep AL strategies is often greatly reduced when deployed in combination with semi-supervised learning. Despite this, we observe that ADA-CLUE provides consistent improvements over uniform sampling on most shifts, even in the presence of strong semi-supervised alignment. This offers encouraging evidence that there remains value in intelligently sampling instances for labeling even with semi-supervised deep learning.

4.2. Ablating ADA-CLUE

Active sampling ablation. To understand the impact of our active sampling method CLUE, we consider fixing the semi-

Training	AL Strategy	R → C			C → S			S → P			C → Q			AVG		
		1k	2k	5k												
ft from source	uniform	51.5	55.3	60.6	42.1	44.4	47.0	41.1	43.8	47.2	23.3	28.1	35.3	39.5	42.9	47.5
	entropy [53]	48.1	52.1	58.6	41.1	42.7	45.7	41.2	43.8	47.2	21.9	26.4	34.0	38.1	41.3	46.4
	margin [37]	51.0	54.8	60.7	42.3	44.3	47.0	41.4	44.0	47.1	23.6	28.4	35.8	39.6	42.9	47.7
	coreset [42]	50.0	54.0	59.6	41.2	42.8	44.9	40.1	42.2	45.4	22.4	26.0	32.4	38.4	41.3	45.6
	BADGE [2]	52.4	56.1	61.7	42.8	45.2	48.1	41.7	44.9	47.9	23.1	28.2	35.5	39.8	43.6	48.3
	CLUE (Ours)	52.9	57.1	62.0	43.3	45.8	48.6	42.4	45.3	48.3	24.3	28.8	35.5	40.7	44.3	48.6
AADA [48]		53.2	57.4	62.8	44.8	46.5	49.2	41.3	43.5	46.1	21.9	25.8	32.4	40.3	43.3	47.6

Table 1: Comparing CLUE against prior AL strategies across 2 learning scenarios: finetuning (ft) from a source model, and semi-supervised DA (using MME [40]) starting from a source model.

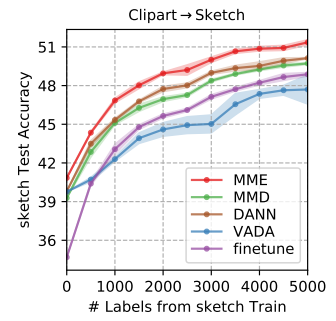


Figure 5: C→S: Varying DA method while sampling via CLUE.

supervised domain adaptation method from our full method, ADA-CLUE, and varying the active sampling method using 4 diverse AL strategies from prior work. Labels are acquired based on the following selection strategies: 1) entropy [53]: Instances over which the model has highest predictive entropy. 2) margin [37]: Instances for which the score difference between the model’s top-2 predictions is the smallest. 3) Coreset [42]: Core-set formulates active sampling as a set-cover problem, and solves the K-Center [54] problem. In our experiments, we use the greedy version proposed in Sener et al. [42]. 4) BADGE [2] (described in Sec. 4.1). Strategies (1) and (2) are purely uncertainty based, (3) is purely diversity-based, and (4) is a hybrid approach.

We evaluate all sampling strategies across two different ways of learning with the acquired labeled data – fine-tuning a model trained on the source domain, and semi-supervised domain alignment via minimax entropy [40] (Eq. 7). AADA [48] is ill-defined in both these settings since it uses a domain classifier to select samples, but for completeness we also report its performance with DANN [13]. We follow the same experimental protocol as before, but report performance only at 3 budgets (1k, 2k, and 5k) for conciseness (full plots in appx.). See Table 1. We observe:

▷ **CLUE outperforms prior work.** In both learning settings, and across most shift difficulties except at the last round on R→C, CLUE performs best. We note here that DomainNet is a complex and large benchmark with 345 categories, which sometimes leads to relatively small margins of improvement.

▷ **Hybrid approaches (CLUE and BADGE) are versatile across shift difficulties.** Approaches solely based on uncertainty work well on relatively easier shifts (R→C), but overall we find purely uncertainty-based (margin, entropy), and diversity-based (coreset) approaches to struggle to generalize to challenging shifts (S→P, C→Q), sometimes underperforming even random sampling! On the other hand, hybrid approaches that combine uncertainty and diversity generalize across shifts.

▷ **Unlabeled data helps in the active DA setting.** Across AL methods, we observe adaptation with MME to consistently outperform finetuning (by 2.4-2.7% accuracy).

Domain adaptation ablation. We next justify our decision to use MME as our semi-supervised domain adaptation method. For this experiment, we fix our sampling strategy to CLUE and compare against: i) MMD [28], a discrepancy-statistic based DA method, ii) Two domain-classifier based DA methods: DANN [14] and VADA [45], and iii) standard finetuning. In Fig. 5, we observe that domain alignment with MME significantly outperforms all alternative domain adaptation methods as well as finetuning. With all DA methods except VADA, we observe improvements over finetuning; however, MME clearly performs best. This finding is consistent with Saito *et al.* [40], who find that domain-classifier based methods are not as effective in the semi-supervised setting when additional target labels are available.

Visualizing CLUE. Finally, we provide an illustrative comparison of sampling strategies using t-SNE [29]. Fig. 6 shows an initial feature landscape together with points selected by entropy, coresnet, and CLUE at Round 0 on the SVHN→MNIST shift. We find that entropy (*left*) samples uncertain but redundant points, coresnet samples diverse but not necessarily uncertain points, while our method, CLUE, samples both diverse and uncertain points. In appx., we include additional experiments such as varying label budgets and numbers of Active DA rounds, and find CLUE to consistently provide improvements across settings.

4.3. Additional Analysis

Time complexity. Table 2 shows average case complexity and time-per-round for our primary experiments. Methods are ordered by average performance (Fig 4): CLUE and BADGE achieve the best accuracy but are slower due to a CPU clustering step. CLUE can be optimized further via GPU acceleration, using last-(instead of penultimate) layer embeddings, or pre-filtering data before clustering.

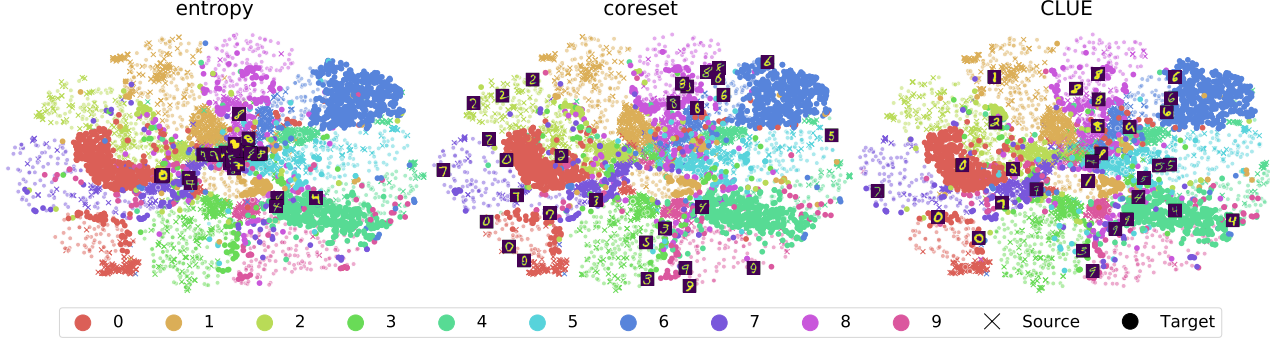


Figure 6: SVHN → MNIST: We visualize the logits of a subset of incorrect (large, opaque circles) and correct (partly transparent circles) model predictions on the target domain after round 0, along with examples sampled by different methods. Entropy (left) acquires redundant samples, whereas core-set (middle) does not account for areas of the feature space that are already well understood. CLUE (right) constructs batches of dissimilar samples from dense regions with high uncertainty.

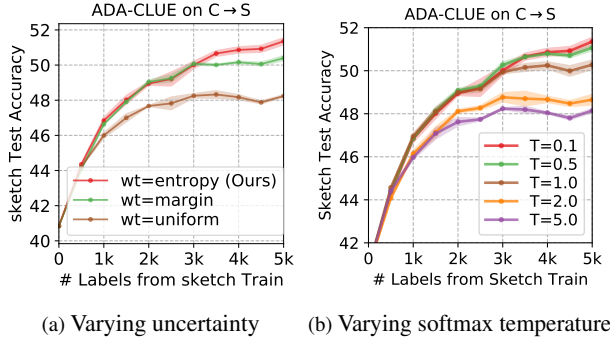


Figure 7: Ablating CLUE on DomainNet C → S

Varying uncertainty measure in CLUE. In Fig. 7a, we consider alternative uncertainty measures for CLUE on the C → S shift. We show that our proposed use of sample entropy significantly outperforms a uniform sample weight and slightly outperforms an alternative uncertainty measure - sample margin score (difference between scores for top-2 most likely classes). This illustrates the importance of using uncertainty-weighting to bias CLUE towards informative samples. It also shows that predictive entropy carries useful signal for instance selection even in the present of minimax entropy optimization. We also run an additional experiment (not shown) where we use embeddings from the last CNN layer (instead of penultimate) CLUE, and observe near-identical performance across multiple shifts, suggesting that our method is not very sensitive to this choice.

Varying trade-off between uncertainty and diversity. In Fig. 7b we run a sweep over temperature values used for CLUE on C → S. As seen, lower values of temperature appear to improve performance, particularly at later rounds when uncertainty estimates are more reliable.

How well does CLUE learn from scratch? While CLUE is designed as an Active DA strategy, we also evaluate its

	AL Strategy	Query Complexity	Query Time (DIGITS, C → S)
fwd + cluster	CLUE	$\mathcal{O}(tNBD)$	(60s, 16.2m)
	BADGE	$\mathcal{O}(NBDC)$	(103s, 16.3m)
	coreset	$\mathcal{O}(CNB)$	(52s, 2.8m)
fwd + rank	AADA	$\mathcal{O}(NC)$	(3.7s, 139s)
	entropy	$\mathcal{O}(NC)$	(3.5s, 45s)
	margin	$\mathcal{O}(NC)$	(3.2s, 45s)

Table 2: Query complexity and time per round for CLUE compared to other AL strategies. C and N denotes number of classes and instances respectively, D denotes embedding dimensionality, B denotes budget, t = iterations, and fwd stands for forward pass.

performance against prior work when learning from “scratch” as is conventional in AL. We find it to outperform prior work when finetuning using ImageNet [38] initialization on C → S, and perform on par with competing methods when finetuning from scratch on SVHN [31]. See appx. for additional details.

5. Conclusion

We address active domain adaptation, where the task is to generalize a source model to an unlabeled target domain by acquiring labels for selected target instances via an oracle. We present ADA-CLUE, an algorithm for active domain adaptation that first identifies diverse instances from the target domain for labeling that are both uncertain under the model and representative of target data, and then optimizes a semi-supervised adversarial entropy loss to induce domain alignment. We demonstrate its effectiveness on the Active DA task against competing active learning, semi-supervised domain adaptation, and active adaptation methods across domain shifts of varying difficulty.

References

[1] David Arthur and Sergei Vassilvitskii. k-means++: The advantages of careful seeding. Technical report, Stanford, 2006. 6

[2] Jordan T Ash, Chicheng Zhang, Akshay Krishnamurthy, John Langford, and Alekh Agarwal. Deep batch active learning by diverse, uncertain gradient lower bounds. In *International Conference on Learning Representations*, 2020. 1, 2, 3, 5, 6, 7, 11, 12

[3] Yoram Baram, Ran El Yaniv, and Kobi Luz. Online choice of active learning algorithms. *Journal of Machine Learning Research*, 5(Mar):255–291, 2004. 2

[4] Klaus Brinker. Incorporating diversity in active learning with support vector machines. In *Proceedings of the 20th international conference on machine learning (ICML-03)*, pages 59–66, 2003. 5

[5] Rita Chattpadhyay, Wei Fan, Ian Davidson, Sethuraman Panchanathan, and Jieping Ye. Joint transfer and batch-mode active learning. In *International Conference on Machine Learning*, pages 253–261, 2013. 2

[6] Wei-Yu Chen, Yen-Cheng Liu, Zsolt Kira, Yu-Chiang Wang, and Jia-Bin Huang. A closer look at few-shot classification. In *International Conference on Learning Representations*, 2019. 15

[7] David Cohn, Les Atlas, and Richard Ladner. Improving generalization with active learning. *Machine learning*, 15(2):201–221, 1994. 1

[8] A David. Vassilvitskii s.: K-means++: The advantages of careful seeding. In *18th annual ACM-SIAM symposium on Discrete algorithms (SODA), New Orleans, Louisiana*, pages 1027–1035, 2007. 11, 12

[9] Jeff Donahue, Judy Hoffman, Erik Rodner, Kate Saenko, and Trevor Darrell. Semi-supervised domain adaptation with instance constraints. In *Proceedings of the IEEE conference on computer vision and pattern recognition*, pages 668–675, 2013. 1, 2

[10] Melanie Ducoffe and Frederic Precioso. Adversarial active learning for deep networks: a margin based approach. *arXiv preprint arXiv:1802.09841*, 2018. 1, 2

[11] Charles Elkan. Using the triangle inequality to accelerate k-means. In *Proceedings of the 20th international conference on machine learning (ICML-03)*, pages 147–153, 2003. 12

[12] Yarin Gal, Riashat Islam, and Zoubin Ghahramani. Deep bayesian active learning with image data. In *Proceedings of the 34th International Conference on Machine Learning - Volume 70*, pages 1183–1192. JMLR. org, 2017. 1, 2

[13] Yaroslav Ganin and Victor Lempitsky. Unsupervised domain adaptation by backpropagation. In *International Conference on Machine Learning*, pages 1180–1189, 2015. 1, 2, 7

[14] Yaroslav Ganin, Evgeniya Ustinova, Hana Ajakan, Pascal Germain, Hugo Larochelle, François Laviolette, Mario Marchand, and Victor Lempitsky. Domain-adversarial training of neural networks. *The Journal of Machine Learning Research*, 17(1):2096–2030, 2016. 2, 6, 7

[15] Yonatan Geifman and Ran El-Yaniv. Deep active learning over the long tail. *arXiv preprint arXiv:1711.00941*, 2017. 2

[16] Daniel Gissin and Shai Shalev-Shwartz. Discriminative active learning. *arXiv preprint arXiv:1907.06347*, 2019. 2

[17] Greg Hamerly and Charles Elkan. Alternatives to the k-means algorithm that find better clusterings. In *Proceedings of the eleventh international conference on Information and knowledge management*, pages 600–607, 2002. 12

[18] John A Hartigan and Manchek A Wong. Algorithm as 136: A k-means clustering algorithm. *Journal of the Royal Statistical Society. Series C (Applied Statistics)*, 28(1):100–108, 1979. 2

[19] Kaiming He, Xiangyu Zhang, Shaoqing Ren, and Jian Sun. Deep residual learning for image recognition. In *Proceedings of the IEEE conference on computer vision and pattern recognition*, pages 770–778, 2016. 5, 11, 12

[20] Judy Hoffman, Eric Tzeng, Taesung Park, Jun-Yan Zhu, Phillip Isola, Kate Saenko, Alexei Efros, and Trevor Darrell. Cycada: Cycle-consistent adversarial domain adaptation. In *International Conference on Machine Learning*, pages 1989–1998, 2018. 1, 2, 5, 12

[21] Wei-Ning Hsu and Hsuan-Tien Lin. Active learning by learning. In *Twenty-Ninth AAAI conference on artificial intelligence*, 2015. 2

[22] Joshua Zhixue Huang, Michael K Ng, Hongqiang Rong, and Zichen Li. Automated variable weighting in k-means type clustering. *IEEE transactions on pattern analysis and machine intelligence*, 27(5):657–668, 2005. 4

[23] Diederik P Kingma and Jimmy Ba. Adam: A method for stochastic optimization. *arXiv preprint arXiv:1412.6980*, 2014. 12

[24] Andreas Kirsch, Joost van Amersfoort, and Yarin Gal. Batchbald: Efficient and diverse batch acquisition for deep bayesian active learning. In *Advances in Neural Information Processing Systems*, pages 7024–7035, 2019. 1

[25] Hans-Peter Kriegel, Erich Schubert, and Arthur Zimek. The (black) art of runtime evaluation: Are we comparing algorithms or implementations? *Knowledge and Information Systems*, 52(2):341–378, 2017. 4

[26] Yann LeCun, Léon Bottou, Yoshua Bengio, and Patrick Haffner. Gradient-based learning applied to document recognition. *Proceedings of the IEEE*, 86(11):2278–2324, 1998. 2, 5, 6, 11

[27] Mingsheng Long, Yue Cao, Jianmin Wang, and Michael Jordan. Learning transferable features with deep adaptation networks. In *International Conference on Machine Learning*, pages 97–105, 2015. 2

[28] Mingsheng Long, Jianmin Wang, Guiguang Ding, Jiaguang Sun, and Philip S Yu. Transfer feature learning with joint distribution adaptation. In *Proceedings of the IEEE international conference on computer vision*, pages 2200–2207, 2013. 7

[29] Laurens van der Maaten and Geoffrey Hinton. Visualizing data using t-sne. *Journal of machine learning research*, 9(Nov):2579–2605, 2008. 7, 13

[30] Sudhanshu Mittal, Maxim Tatarchenko, Özgün Çiçek, and Thomas Brox. Parting with illusions about deep active learning. *arXiv preprint arXiv:1912.05361*, 2019. 6

[31] Yuval Netzer, Tao Wang, Adam Coates, Alessandro Bissacco, Bo Wu, and Andrew Y Ng. Reading digits in natural images with unsupervised feature learning. In *Neural Information Processing Systems (NeurIPS)*, 2011. 2, 5, 6, 8, 11

[32] Adam Paszke, Sam Gross, Francisco Massa, Adam Lerer, James Bradbury, Gregory Chanan, Trevor Killeen, Zeming Lin, Natalia Gimelshein, Luca Antiga, et al. Pytorch: An imperative style, high-performance deep learning library. In *Advances in Neural Information Processing Systems*, pages 8024–8035, 2019. [11](#)

[33] Fabian Pedregosa, Gaël Varoquaux, Alexandre Gramfort, Vincent Michel, Bertrand Thirion, Olivier Grisel, Mathieu Blondel, Peter Prettenhofer, Ron Weiss, Vincent Dubourg, et al. Scikit-learn: Machine learning in python. *the Journal of machine Learning research*, 12:2825–2830, 2011. [11](#)

[34] Xingchao Peng, Qinxun Bai, Xide Xia, Zijun Huang, Kate Saenko, and Bo Wang. Moment matching for multi-source domain adaptation. In *Proceedings of the IEEE International Conference on Computer Vision*, pages 1406–1415, 2019. [2](#), [5](#), [6](#), [11](#), [13](#)

[35] George R Price. Extension of covariance selection mathematics. *Annals of human genetics*, 35(4):485–490, 1972. [4](#), [14](#)

[36] Piyush Rai, Avishek Saha, Hal Daumé III, and Suresh Venkatasubramanian. Domain adaptation meets active learning. In *Proceedings of the NAACL HLT 2010 Workshop on Active Learning for Natural Language Processing*, pages 27–32. Association for Computational Linguistics, 2010. [1](#), [2](#)

[37] Dan Roth and Kevin Small. Margin-based active learning for structured output spaces. In *European Conference on Machine Learning*, pages 413–424. Springer, 2006. [2](#), [7](#)

[38] Olga Russakovsky, Jia Deng, Hao Su, Jonathan Krause, Sanjeev Satheesh, Sean Ma, Zhiheng Huang, Andrej Karpathy, Aditya Khosla, Michael Bernstein, et al. Imagenet large scale visual recognition challenge. *International journal of computer vision*, 115(3):211–252, 2015. [8](#), [11](#)

[39] Kate Saenko, Brian Kulis, Mario Fritz, and Trevor Darrell. Adapting visual category models to new domains. In *European conference on computer vision*, pages 213–226. Springer, 2010. [1](#), [2](#), [5](#), [6](#)

[40] Kuniaki Saito, Donghyun Kim, Stan Sclaroff, Trevor Darrell, and Kate Saenko. Semi-supervised domain adaptation via minimax entropy. In *Proceedings of the IEEE International Conference on Computer Vision*, pages 8050–8058, 2019. [1](#), [2](#), [4](#), [5](#), [6](#), [7](#), [15](#)

[41] Greg Schohn and David Cohn. Less is more: Active learning with support vector machines. In *ICML*, volume 2, page 6. Citeseer, 2000. [2](#)

[42] Ozan Sener and Silvio Savarese. Active learning for convolutional neural networks: A core-set approach. In *International Conference on Learning Representations*, 2018. [1](#), [2](#), [3](#), [7](#)

[43] Burr Settles. Active learning literature survey. Technical report, University of Wisconsin-Madison Department of Computer Sciences, 2009. [1](#)

[44] Hidetoshi Shimodaira. Improving predictive inference under covariate shift by weighting the log-likelihood function. *Journal of statistical planning and inference*, 90(2):227–244, 2000. [1](#)

[45] Rui Shu, Hung H Bui, Hirokazu Narui, and Stefano Ermon. A dirt-t approach to unsupervised domain adaptation. In *Proc. 6th International Conference on Learning Representations*, 2018. [7](#)

[46] Samarth Sinha, Sayna Ebrahimi, and Trevor Darrell. Variational adversarial active learning. In *Proceedings of the IEEE International Conference on Computer Vision*, pages 5972–5981, 2019. [2](#)

[47] Jasper Snoek, Yaniv Ovadia, Emily Fertig, Balaji Lakshminarayanan, Sebastian Nowozin, D Sculley, Joshua Dillon, Jie Ren, and Zachary Nado. Can you trust your model’s uncertainty? evaluating predictive uncertainty under dataset shift. In *Advances in Neural Information Processing Systems*, pages 13969–13980, 2019. [2](#), [3](#), [15](#)

[48] Jong-Chyi Su, Yi-Hsuan Tsai, Kihyuk Sohn, Buyu Liu, Subhransu Maji, and Manmohan Chandraker. Active adversarial domain adaptation. In *The IEEE Winter Conference on Applications of Computer Vision*, pages 739–748, 2020. [2](#), [3](#), [5](#), [6](#), [7](#), [12](#)

[49] Simon Tong and Daphne Koller. Support vector machine active learning with applications to text classification. *Journal of machine learning research*, 2(Nov):45–66, 2001. [1](#), [2](#)

[50] Antonio Torralba and Alexei A Efros. Unbiased look at dataset bias. In *Proceedings of the IEEE Conference on Computer Vision and Pattern Recognition*, pages 1521–1528. IEEE, 2011. [1](#)

[51] Eric Tzeng, Judy Hoffman, Kate Saenko, and Trevor Darrell. Adversarial discriminative domain adaptation. In *Proceedings of the IEEE Conference on Computer Vision and Pattern Recognition*, pages 7167–7176, 2017. [2](#)

[52] Eric Tzeng, Judy Hoffman, Ning Zhang, Kate Saenko, and Trevor Darrell. Deep domain confusion: Maximizing for domain invariance. *arXiv preprint arXiv:1412.3474*, 2014. [1](#), [2](#)

[53] Dan Wang and Yi Shang. A new active labeling method for deep learning. In *2014 International joint conference on neural networks (IJCNN)*, pages 112–119. IEEE, 2014. [2](#), [4](#), [7](#)

[54] Gert W Wolf. Facility location: concepts, models, algorithms and case studies. series: Contributions to management science: edited by zanjirani farahani, reza and hekmatfar, masoud, heidelberg, germany, physica-verlag, 2009, 2011. [7](#)

[55] Ting Yao, Yingwei Pan, Chong-Wah Ngo, Houqiang Li, and Tao Mei. Semi-supervised domain adaptation with subspace learning for visual recognition. In *Proceedings of the IEEE conference on Computer Vision and Pattern Recognition*, pages 2142–2150, 2015. [1](#), [2](#)

[56] Yuli Zhang, Huaiyu Wu, and Lei Cheng. Some new deformation formulas about variance and covariance. In *2012 Proceedings of International Conference on Modelling, Identification and Control*, pages 987–992. IEEE, 2012. [4](#), [14](#)

[57] Fedor Zhdanov. Diverse mini-batch active learning. *arXiv preprint arXiv:1901.05954*, 2019. [2](#)

6. Appendix

Contents

6.1. Further Ablations for ADA-CLUE	11
6.1.1 How many Active DA rounds are optimal?	11
6.1.2 Convergence: When do gains saturate?	11
6.2. Performance of CLUE on Standard AL	11
6.3. Dataset details	11
6.4. Additional Implementation Details	11
6.4.1 Baseline Implementations	12
6.5. Understanding ADA-CLUE	13
6.6. Extended Description of the CLUE Objective	14
6.7. ADA-CLUE: Active Sampling Ablation	15

6.1. Further Ablations for ADA-CLUE

6.1.1 How many Active DA rounds are optimal?

Given a fixed total budget of 5000 target labels, we now vary the per round budget (and consequently the total number of active adaptation rounds) and report performance on the Clipart→Sketch shift. As seen in Fig. 8a, the performance appears fairly robust to the per-round budget across values of 500, 1000, and 2500 but suffers at very small budgets (100). We conjecture that this is possibly due to the large number of classes in DomainNet (345), which cannot be adequately represented at such small budgets.

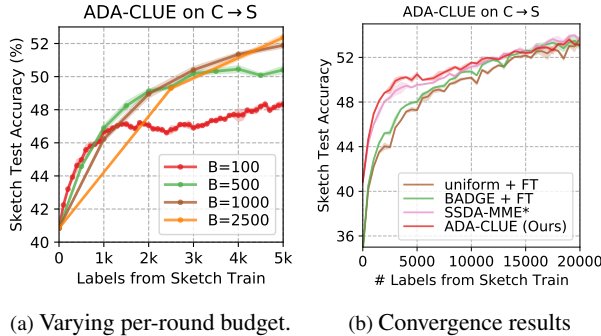


Figure 8: C→S: Additional ADA-CLUE ablations.

6.1.2 Convergence: When do gains saturate?

Due to the computational expense of running active domain adaptation on multiple shifts with a large CNN (ResNet34 [19]) on a large dataset (DomainNet [34]), in the main paper we restrict ourselves to 10 rounds with a per-round budget of 500. As a check on when performance gains saturate, we benchmark performance on Clipart→Sketch for 40 rounds with per-round budget of 500 (= 20k labels in total). Results are presented in Fig. 8b. As seen, performance

begins to roughly saturate around the 15k labels mark, and performance differences across methods narrow.

6.2. Performance of CLUE on Standard AL

While CLUE is designed as an Active DA strategy, we nevertheless study its suitability for traditional active learning in which models are typically trained from “scratch”. We benchmark its performance against competing methods in two settings: Finetuning from an ImageNet [38] initialization on the Clipart→Sketch shift from DomainNet, following the same experimental protocol we use for Active DA (but set softmax temperature $T=1.0$ as uncertainty is less reliable when learning from scratch), and the standard SVHN benchmark used for active learning [2]. For AL on SVHN, we match the setting in Ash *et al.* [2], initializing a ResNet18 [19] CNN with random weights and perform 100 rounds of active learning with per-round budget of 100. As summarized in Figure 9a, on DomainNet CLUE significantly outperforms prior work. On SVHN (Fig 9b), CLUE is on-par with state-of-the-art AL methods, and statistically significantly better than uniform sampling over most rounds.

6.3. Dataset details

DomainNet. For our primary experiments, we use the DomainNet [34] dataset that consists of 0.6 million images spanning 6 domains, available at <http://ai.bu.edu/M3SDA/>. For our experiments, we use 4 shifts from 5 domains: Real, Clipart, Sketch, Painting, and Quickdraw. Table 3 summarizes the train/test statistics of each of these domains, while Fig. 11 provides representative examples from each. As models use ImageNet initialization, we avoid using Real as a target domain.

	Real	Clipart	Painting	Sketch	Quickdraw
Train	120906	33525	48212	50416	120750
Test	52041	14604	20916	21850	51750

Table 3: DomainNet [34] train/test statistics

DIGITS. We present results on the SVHN [31]→MNIST [26] domain shift. Both datasets consist of images of the digits 0-9. SVHN consists of 99289 (73257 train, 26032 test) RGB images whereas MNIST contains 70k (60k train, 10k test) grayscale images. Fig. 10 shows representative examples.

6.4. Additional Implementation Details

We use PyTorch [32] for all our experiments. Most experiments were run on an NVIDIA TitanX GPU.

CLUE. We use the weighted K-Means implementation in scikit-learn [33] to implement CLUE. Cluster centers are initialized via K-means++ [8]. The implementation uses

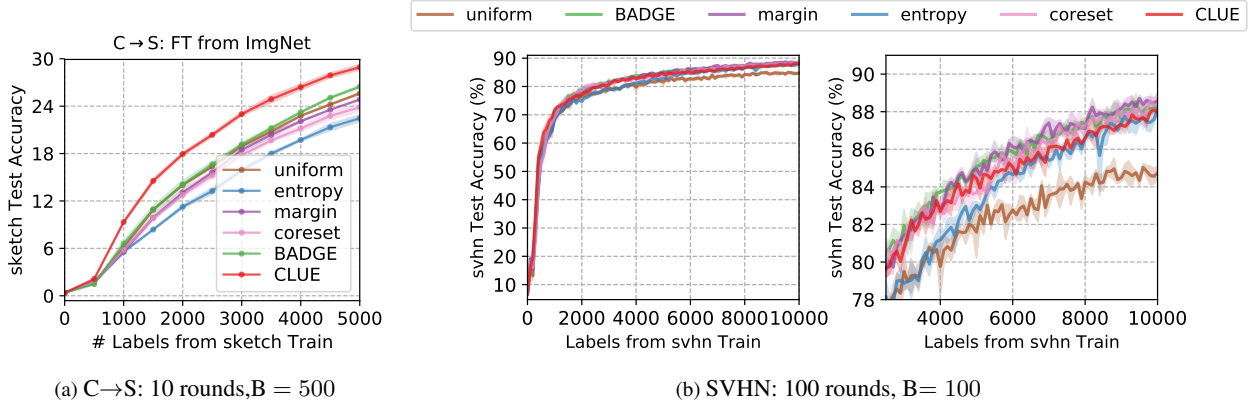


Figure 9: Active learning performance of CLUE on DomainNet C→S (finetuning from ImageNet initialization) and SVHN (finetuning from scratch). CLUE significantly outperforms state-of-the-art active learning methods in the first case and performs on-par in the second.

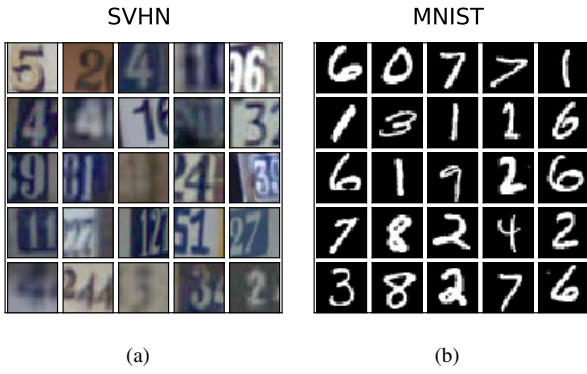


Figure 10: DIGITS qualitative examples

the Elkan algorithm [17] to solve K-Means. For n objects, k clusters, and e iterations ($= 300$ in our experiments), the time complexity of the Elkan algorithm is roughly $\mathcal{O}(nke)$ [11], while its space complexity is $\mathcal{O}(nk)$.

DomainNet experiments. We utilize a ResNet34 [19] CNN architecture. For active adaptation (round 1 and onwards), we use the Adam [23] optimizer with a learning rate of 10^{-5} , weight decay of 10^{-5} and train for 20 epochs per round (with an epoch defined as a complete pass over labeled target data) with a batch size of 64. For unsupervised adaptation (round 0), we use Adam with a learning rate of 3×10^{-7} , weight decay of 10^{-5} , and train for 50 epochs. Across all adaptation methods, we tune loss weights to ensure that the average labeled loss is approximately 10 times as large as the average unsupervised loss. We use random cropping and random horizontal flips for data augmentation. We set loss weights $\lambda_S = 0.1$, $\lambda_T = 1$ and $\lambda_H = 0.1$ (Section 3).

Tuning softmax temperature. In Active DA, it is unrealistic to assume access to a large labeled validation set on the target to tune hyperparameters. To tune the softmax temperature hyperparameter for CLUE that trades off uncertainty and

diversity, we thus create a small heldout validation set of 1% of target data (482 examples) on the Clipart→Sketch shift, and perform a grid search over temperature values. We select $T = 0.1$ based on its relatively consistent performance across rounds. As shown in Fig.7 (b) in the main paper, we find this parameter to also translate to good performance on the target test set.

DIGITS experiments. We use the modified LeNet architecture proposed in Hoffman et al. [20] and exactly match the experimental setup in AADA [48]. We use the Adam [23] optimizer with a learning rate of 2×10^{-4} , weight decay of 10^{-5} , batch size of 128, and perform 60 epochs of training per-round. We halve the learning rate every 20 epochs. We set loss weights $\lambda_S = 0.1$, $\lambda_T = 1$ and $\lambda_H = 1$ (Section 3).

6.4.1 Baseline Implementations

We elaborate on our implementation of the BADGE [2] and AADA [48] baselines.

BADGE. BADGE “gradient embeddings” are computed by taking the gradient of model loss with respect to classifier weights, where the loss is computed as cross-entropy between the model’s predictive distribution and its most confidently predicted class. Next, K-Means++ [8] is run on these embeddings to yield a batch of samples.

AADA. In AADA, a domain discriminator G_d is learned to distinguish between source and target features obtained from an extractor G_f , in addition to a task classifier G_y . For active

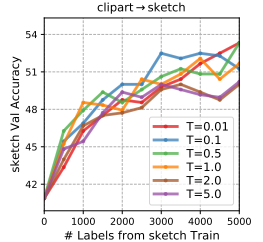


Figure 12: C→S: Tuning softmax temperature with a small target validation set (1% data).

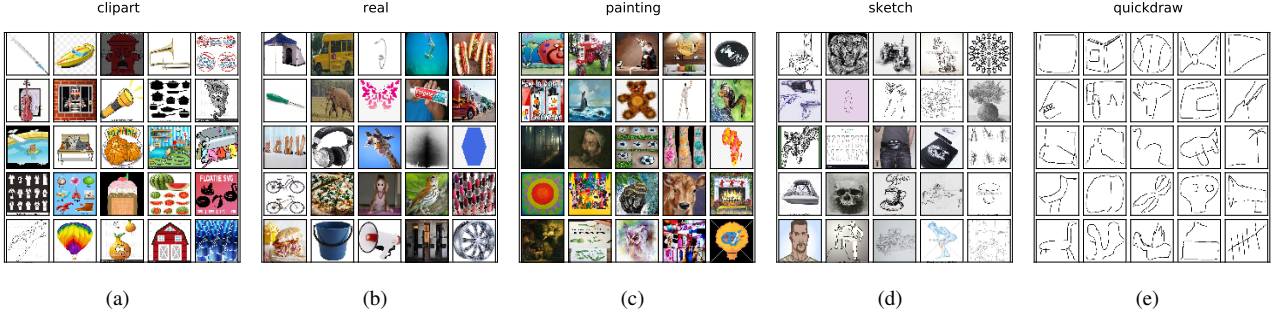


Figure 11: DomainNet [34] qualitative examples

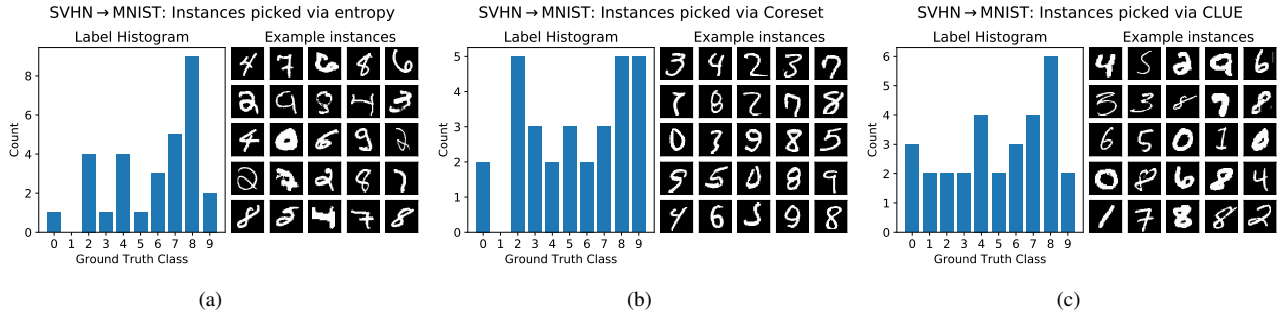


Figure 13: SVHN → MNIST: Label histograms and examples of instances selected by entropy, coresnet, and CLUE at Round 1 with $B = 30$.

sampling, points are scored via the following importance weighting-based acquisition function (\mathcal{H} denotes model entropy): $s(x) = \frac{1-G_d(G_f(x))}{G_d^*(G_f(x))} \mathcal{H}(G_y(G_f(x)))$, and top B instances are selected for labeling. In practice, to generate less redundant batches we randomly sample B instances from the top-2% scores, as recommended by the authors. Consistent with the original work, we also add an entropy minimization objective with a loss weight of 0.01.

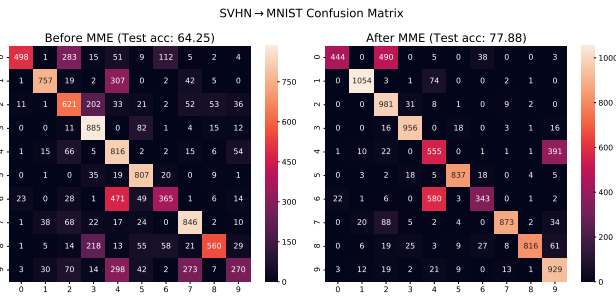


Figure 15: SVHN → MNIST: Confusion matrix of model predictions before and after MME at round 0.

6.5. Understanding ADA-CLUE

We attempt to get a sense of the behavior of ADA-CLUE versus other methods via visualizations on the SVHN → MNIST shift. Fig. 15 shows confusion matrices of model predictions before (*left*) and after (*right*) performing

unsupervised adaptation (via MME) at round 0. As seen, MME aligns some classes (eg. 1's and 9's) remarkably well even without access to target labels. However, large misalignments remain for some other classes (0, 4, and 6).

Visualizing selected points. In Fig. 13, we visualize instances selected by three strategies at Round 0 – entropy, coresnet, and CLUE, with $B = 30$. We visualize the ground truth label distribution of the selected instances, as well as qualitative examples. As seen, strategies vary across methods. ‘Entropy’ tends to pick a large number of 8’s, and selects high-entropy examples that (on average) appear challenging even to humans. ‘Coreset’ tends to have a wider spread over classes. CLUE appears to interpolate between the behavior of these two methods, selecting a large number of 8’s (like entropy) but also managing to sample atleast a few instances from every class (like coresnet).

t-SNE visualization over rounds. In Fig. 14, we illustrate the sampling behavior of CLUE over rounds via t-SNE [29] visualizations. We follow the same conventions as Fig.6 of the main paper, and visualize the logits of a subset of incorrect (large, opaque circles) and correct (partly transparent circles) model predictions on the target domain, along with instances sampled via CLUE. We oversample incorrect target predictions to emphasize regions of the feature space on which the model currently underperforms. Across all four stages, we find that ADA-CLUE samples instances that are uncertain (often present in a cluster of incorrectly classified

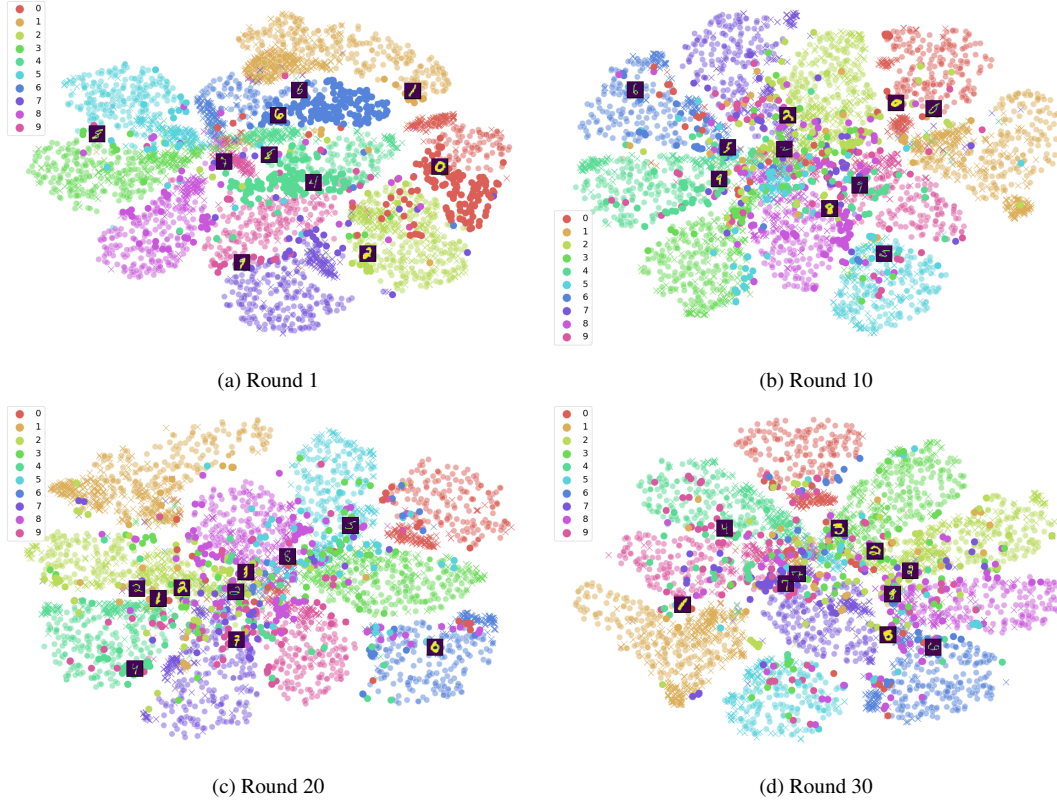


Figure 14: SVHN→MNIST: TSNE visualization of feature space and instances picked by CLUE at rounds 1, 10, 20, and 30. Circles denote target points and crosses denote source points.

instances) and diverse in feature space. This behavior is seen even at later rounds when classes appear better separated.

6.6. Extended Description of the CLUE Objective

We describe in more detail the CLUE objective presented in the main paper. Recall that we seek to identify target instances that are diverse in model feature space. Considering the L_2 distance in the CNN representation space $\phi(\cdot)$ as a dissimilarity measure, we quantify dissimilarity between instances within a set X_k in terms of its variance $\sigma^2(X_k)$ [56]:

$$\begin{aligned} \sigma^2(X_k) &= \frac{1}{2|X_k|^2} \sum_{\mathbf{x}_i, \mathbf{x}_j \in X_k} \|\phi(\mathbf{x}_i) - \phi(\mathbf{x}_j)\|^2 \\ &= \frac{1}{|X_k|} \sum_{\mathbf{x} \in X_k} \|\phi(\mathbf{x}) - \mu_k\|^2 \end{aligned} \quad (8)$$

$$\text{where } \mu_k = \frac{1}{|X_k|} \sum_{\mathbf{x} \in X_k} \phi(\mathbf{x})$$

A small $\sigma^2(X_k)$ indicates that a set X_k contains instances that are similar to one other. Our goal is to identify sets of instances that are representative of the unlabeled target set, by partitioning the unlabeled target data into K sets, each with

small $\sigma^2(X_k)$. Formulating this as a set-partitioning problem with partition function $\mathcal{S} : X_T \rightarrow \{X_1, X_2, \dots, X_K\}$, we seek to find the \mathcal{S} that minimizes the sum of variance over all sets $\sum_{k=1}^N \sigma^2(X_k)$.

To ensure that the more informative/uncertain instances play a larger role in identifying representative instances, we employ weighted-variance, where an instance is weighted by its informativeness. Let h_i denote the scalar weight corresponding to the instance \mathbf{x}_i . The weighted variance [35] $\sigma_{\mathcal{H}}^2(X_k)$ of a set of instances is given by:

$$\begin{aligned} \sigma_{\mathcal{H}}^2(X_k) &= \frac{1}{\sum_{\mathbf{x}_i \in X_k} h_i} \sum_{\mathbf{x}_i \in X_k} h_i \|\phi(\mathbf{x}_i) - \mu_k\|^2 \\ \text{where } \mu_k &= \frac{1}{\sum h_i} \sum_{\mathbf{x}_i \in X_k} h_i \phi(\mathbf{x}_i) \end{aligned} \quad (9)$$

Considering the informativeness (weight) of an instance to be its uncertainty under the model, given by $\mathcal{H}(Y|\mathbf{x})$ (defined in Eq. 1 in main paper), we rewrite the set-partitioning objective to minimize sum of weighted variance of a set

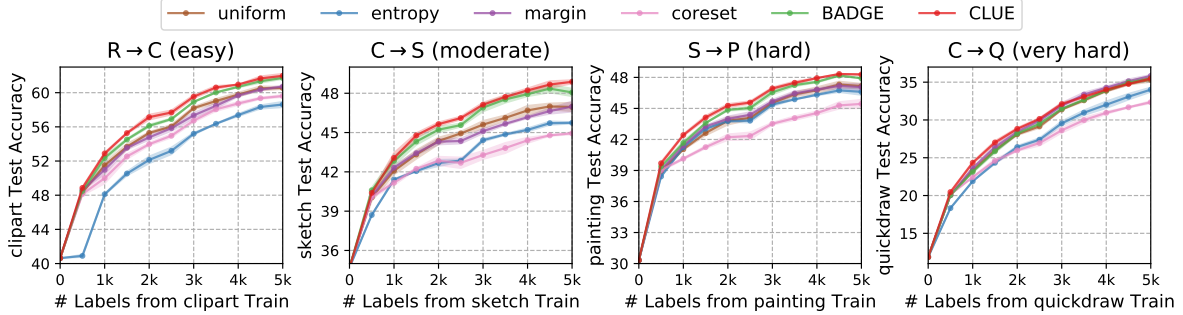


Figure 16: Active Sampling Ablations on DomainNet: Finetuning (FT) from source

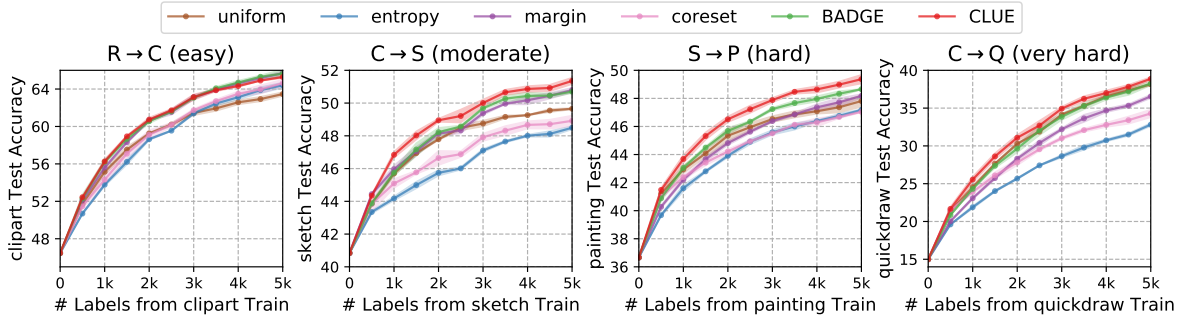


Figure 17: Active Sampling Ablations on DomainNet: Semi-supervised DA (via MME) from source

(from Eq. 9):

$$\begin{aligned}
 & \underset{\mathcal{S}}{\operatorname{argmin}} \sum_{k=1}^K \sigma_{\mathcal{H}}^2(X_k) \\
 &= \underset{\mathcal{S}}{\operatorname{argmin}} \sum_{k=1}^K \frac{1}{Z_k} \sum_{\mathbf{x} \in X_k} \mathcal{H}(Y|\mathbf{x}) \|\phi(\mathbf{x}) - \mu_k\|^2 \\
 & \text{where } \mu_k = \frac{1}{\sum_{x \in X_k} \mathcal{H}(Y|\mathbf{x})} \sum_{\mathbf{x} \in X_k} \mathcal{H}(Y|\mathbf{x}) \phi(\mathbf{x}) \\
 & \text{and } Z_k = \sum_{x \in X_k} \mathcal{H}(Y|\mathbf{x})
 \end{aligned} \tag{10}$$

This, gives us the overall set-partitioning objective for CLUE. (Eq. 4 in main paper).

6.7. ADA-CLUE: Active Sampling Ablation

In Table 1 of the main paper, we presented ablations of ADA-CLUE where we kept the learning strategy fixed (to finetuning (FT) a source model, and semi-supervised DA via MME starting from a source model respectively). For conciseness we presented performance at 3 out of 10 sampling budgets. In Figs. 16, 17, we present the complete learning curves corresponding at all 10 budgets over 3 runs.

7. Future Work

Our work suggests a few promising directions of future work. First, one could experiment with alternative uncertainty measures in ADA-CLUE instead of model entropy, including those (such as uncertainty from deep ensembles) that have been shown to be more reliable under a dataset shift [47]. Further, one could incorporate specialized model architectures from few-shot learning [6, 40] to deal with the label sparsity in the target domain. Finally, while we restrict our task to image classification in this paper, it is important to also study active domain adaptation in the context of related tasks such as object detection and semantic segmentation.